ACS OMEGA

Open Access

http://pubs.acs.org/journal/acsodf

Article

Fast Recovery Double-Network Hydrogels Based on Particulate Macro-RAFT Agents

Runda Wang, Yiteng Lei, Tao Zhu, Rong Fan, Zhongying Jiang,* and Jie Sheng*

Cite This: *ACS Omega* 2023, 8, 35619−35627

Read Online

ACCESS | Metrics & More | Article Recommendations | Supporting Information

ABSTRACT: Synthetic hydrogels struggle to match the high strength, toughness, and recoverability of biological tissues under periodic mechanical loading. Although the hydrophobic polymer chain of polystyrene (PS) may initially collapse into a nanosphere upon contact with water, it has the ability to be elongated when it is subjected to an external force. To address this challenge, we employ the reversible addition−fragmentation chain transfer (RAFT) method to design a carboxyl-substituted polystyrene (CPS) which can form a covalently cross-linked network with four-armed amino-terminated polyethylene glycol (4-armed-PEG-NH_2), and a ductile polyacrylamide network is introduced in order to prepare a double-network (DN) hydrogel. Our results demonstrate that the DN hydrogel exhibits exceptional mechanical properties (0.62 kJ m^{-2} fracture energy, 2510.89 kJ m^{-3} toughness, 0.43 MPa strength, and 820% elongation) when a sufficient external force is applied to fracture it. Moreover, when the DN hydrogel is subjected to a 200% strain, it displays superior recoverability (94.5%). This holds a significant potential in enhancing the mechanical performance of synthetic hydrogels and can have wide-ranging applications in fields such as tissue engineering for hydrophobic polymers.

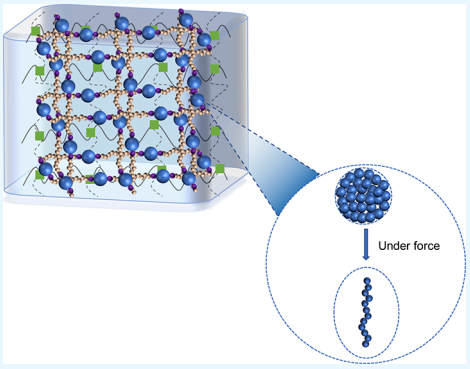

1. INTRODUCTION

Hydrogel is a classical type of polymer with a three-dimensional network structure, which can be water-swollen and absorbs amounts of water, but insoluble in water.[1,2] Therefore, hydrogels are used for tissue engineering,[3−5] as vehicles for drug delivery,[6−8] as biosensors,[9−11] and so forth. However, hydrogels display brittleness and ineffective energy dissipation due to the existence of water,[12] resulting in poor mechanical properties and limiting their wide applications. Many efforts have been devoted to developing high-strength hydrogels by introducing novel network microstructures and cross-linking strategies, such as tetra-polyethylene glycol (PEG) hydrogel,[13−16] slide-ring hydrogel,[17] nanocomposite hydrogel,[18] hydrophobically associated (HA) hydrogel,[19] macromolecular microsphere composite hydrogel,[20] double-network (DN) hydrogel,[2,21,22] and so forth.

In order to address these issues, DN hydrogels are feasible examples that have been used to combine the high mechanical strength and toughness owing to the contrasting network structure and effective energy dissipation.[2,23,24] Specifically, DN hydrogels comprise two covalently linked networks, that is, the first one is rigid and brittle, which maintains the hydrogel shape, and the second is loose and ductile, which fills in the rigid network and absorbs external stress.[23,25,26] For example, alginate−polyacrylamide DN hydrogel can be stretched more than 20 times its original length and has a fracture energy of 9000 J m^{-2}.[27] The hydrogel cannot recover its mechanical properties upon cyclic mechanical loading, if the rigid network, which allows to efficiently dissipate mechanical work and gives rise to high mechanical strength, is ruptured.[23] To overcome such limitations, since the first fully chemical poly(2-acrylamido-2-methylpropanesulfonic acid)/poly(acrylamide) DN hydrogel was invented by Gong et al.,[2] various fully chemical DN hydrogels have obtained attention due to their good mechanical stability,[23] including microgel-reinforced DN hydrogels,[28] void-DN hydrogels,[29] and triple-network hydrogels.[30] These fully chemical DN hydrogels, composed of chemically cross-linked networks, showed excellent tensile stress (0.1−3 MPa), tensile strain (1000−2000%), and high fracture energy (100−1000 J m^{-2}).[26,31] However, due to the irreversible chain breakage of covalent bonds in the rigid and brittle first network, they cannot recover their original conformation after the first loading, which is one of the main limitations for their further applications.

Compared to fully chemical DN hydrogels, hybrid DN hydrogels,[32−35] which consist of physical first network and chemical second network, also display high strength and toughness as well as excellent recovery property from the

Received: March 17, 2023
Accepted: September 8, 2023
Published: September 20, 2023

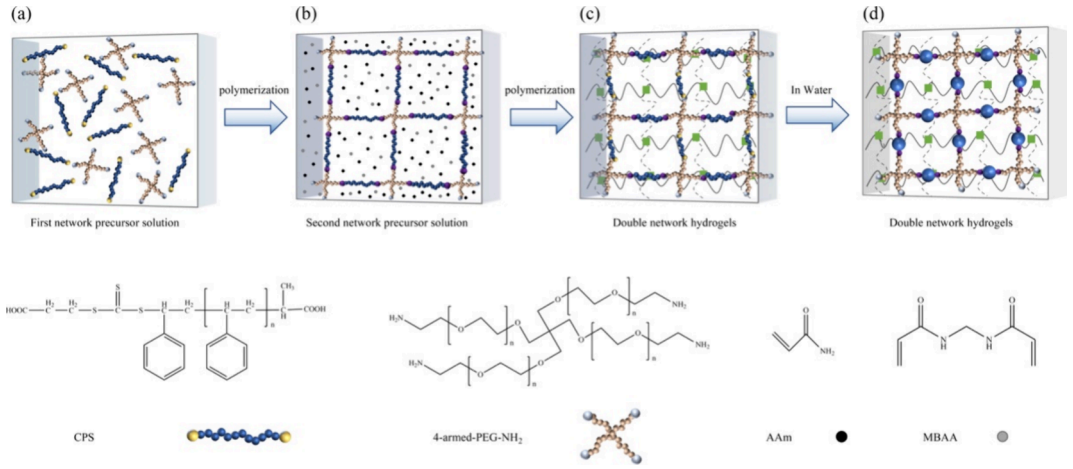

Figure 1. Design and preparation of the PS/PAAm DN hydrogel. (a) In the first network precursor solution, the amino groups (gray balls) on 4-armed-PEG-NH_2 polymer chains form covalent cross-links through the carboxyl groups (yellow balls) on CPS polymer chains. (b) In the second network precursor solution, the first network is joined by covalent cross-links (purple cycles), and the AAm (black points) polymer chains form covalent cross-links through MBAA (gray points). (c) In the PS/PAAm DN hydrogel, the second network is joined by covalent cross-links (green squares), and the two types of polymer network were intertwined. (d) CPSs collapse into nanospheres (blue balls) when the PS/PAAm DN hydrogel is immersed in an amount of deionized water.

loading owing to the reversible physical first network. HA hydrogels refer to physically cross-linked hydrogels formed by hydrophobic interactions and exhibit the enhancement of mechanical strength;[19] hydrophobic interactions are used to construct a sacrificial network to render the DN hydrogels of great mechanical recovery properties.[24] Liu and co-workers first prepared HA hydrogels via using acrylamide (AAm) as the main component and octyl phenol polyethoxy ether as hydrophobic segments.[36] PEG-based polymers have been widely used to prepare covalently cross-linked hydrogels with hydrophobic domains.[13,37,38] Inspired by these hybrid DN hydrogels, we expect to use hydrophobic polymers to design a fully chemically cross-linked DN hydrogel with high mechanical and recovery properties.

In this work, we propose a new kind of method to design a fully chemical DN hydrogel by introducing functional polystyrene (PS). To our knowledge, PS has long been used to process elastomers or textiles.[39−41] Wang has developed a novel nanoparticle-reinforced polyacrylamide-based hydrogel with high mechanical strength (compression strength and tensile strength up to 7.0 and 2.0 MPa), but it has an apparent shortcoming, that is, low stretchability.[42] We have synthesized carboxyl-substituted polystyrene (CPS, 5762 Da) by employing the reversible addition−fragmentation chain transfer (RAFT)[43,44] polymerization method to synthesize the target polymer that possesses the carboxyl group at two termini (Scheme 1, Supporting Information). Weight-average molecular weight (M_w), number-average molecular weight (M_n), and polydispersity of CPS are quantified by gel permeation chromatography (Figure S1, Supporting Information). CPS and four-armed amino-terminated PEG (4-armed-PEG-NH_2, 10000 Da) are chosen to construct the first network (Figure 1a and Scheme 2, Supporting Information); the corresponding network is named PS/PEG single network (SN) hereinafter. Then, by introducing the second network of covalently cross-linked polyacrylamide (PAAm) into the first network (Figure 1b), the stretchable fully chemically cross-linked DN hydrogel is synthesized (Figure 1c), and the corresponding hydrogel is named the PS/PAAm DN hydrogel hereinafter. The chain of the CPS polymer would collapse into a nanosphere when the DN hydrogel is immersed in an amount of deionized water (Figure 1d). The tetra-functionalized PEG is chosen due to its high cross-linking efficiency than that of the bifunctional PEG.[24] By contrast, AAm and N, N′-methylenebis(acrylamide) (MBAA) are chosen to build the second network (Figure 1b and Scheme 3, Supporting Information). Moreover, we have to mention that the cross-linking density for the first and second networks is critical for a notable increase in the mechanical strength of DN hydrogels.[2] A remarkable increase in mechanical strength occurs when the first network is highly cross-linked, and the second one is loosely cross-linked. The chemical structures of AAm, MBAA, CPS, and 4-armed-PEG-NH_2 are shown in Figure 1.

2. EXPERIMENTAL SECTION

2.1. Materials. 2-(2-Carboxyethylsulfanylthiocarbonyl sulfanyl) propionic acid (TTC, Sigma-Aldrich), O-(benzotriazol-1-yl)-N,N,N′,N′-tetra-methyluronium hexafluorophosphate (HBTU, 99%, Aladdin), (3-aminopropyl)triethoxysilane (APTES, 99%, Sigma-Aldrich), N, N-dimethylformamide (DMF, 99.5%, Yasheng Chemical Reagent Co., Ltd.), dimethyl sulfoxide (DMSO, 99.5%, Lingfeng Chemical Reagent Co., Ltd.), triethylamine (TEA, 99.5%, Saen Chemical Reagent Co., Ltd.), methanol (MeOH, 99.5%, Yasheng Chemical Reagent Co., Ltd.), tetrahydrofuran (THF, 99.5%, Lingfeng Chemical Reagent Co., Ltd.), acrylamide (AAm, 99%, General Reagent Co., Ltd.), N,N′-methylenebis(acrylamide) (MBAA, 99%, Aladdin), phenyl bis(2,4,6-trimethylbenzoyl)-phosphine oxide (96%, TCI Chemical Reagent Co., Ltd.), and 4-armed-PEG-NH_2 (95%, Yarebio Chemical Reagent Co., Ltd.) were used as received without further purification. Styrene (St, 99.5%, Aladdin) was dehydrated by alkaline alumina powder at room temperature before use. 2,2′-azobis(2-methyl-propionitrile) (AIBN) was recrystallized from boiling MeOH. DMF and DMSO were stored in sealed bottles.

2.2. Synthesis of CPS. AIBN (14.27 mg, 87 μmol), TTC (110.49 mg, 435 μmol), DMF (300 μL, 3.89 mmol), and freshly distilled St (2.5 mL, 21.63 mmol) were placed in a flame-dried Schlenk tube, and oxygen was removed by three freeze−pump−thaw cycles. The argon-protected Schlenk tube

https://doi.org/10.1021/acsomega.3c01813
ACS Omega 2023, 8, 35619−35627

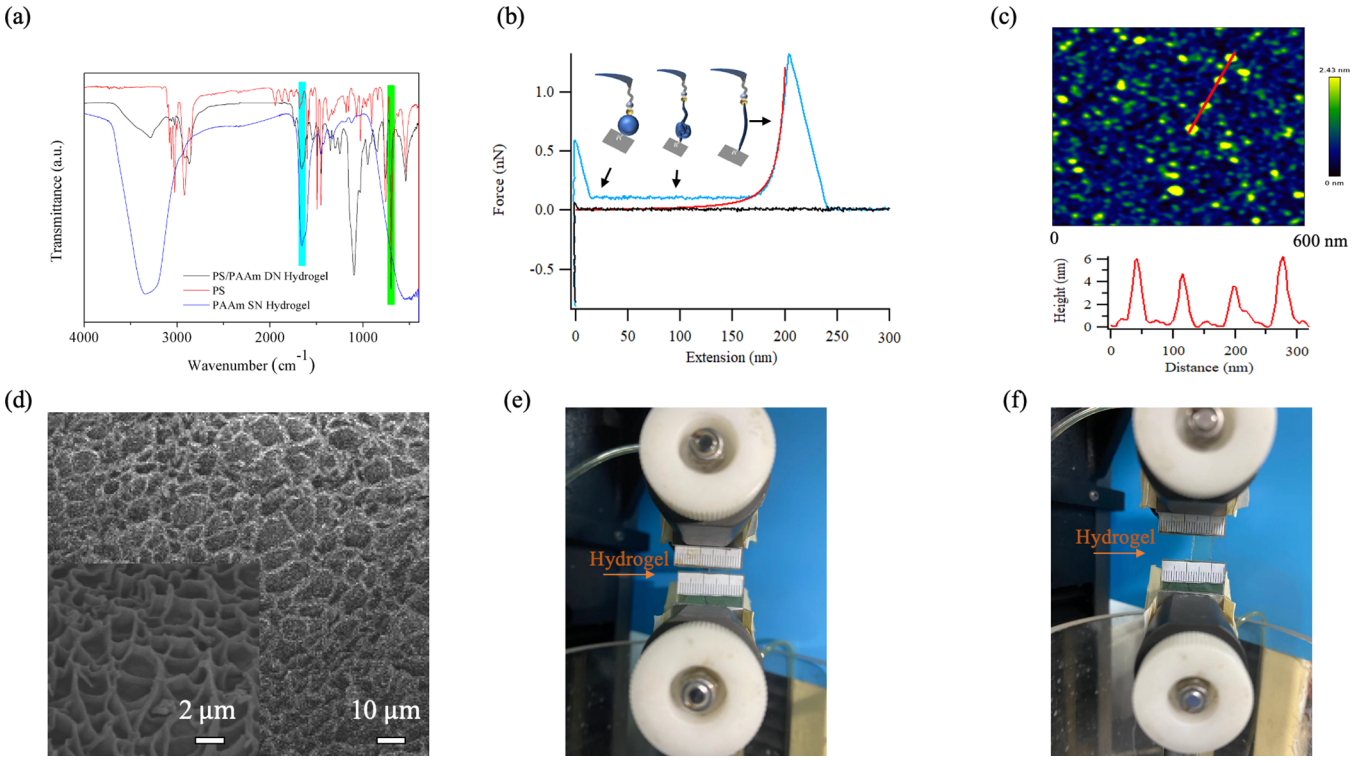

Figure 2. Characterization of the PS/PAAm DN hydrogels. (a) FTIR spectra of the PS/PAAm DN hydrogel and PS and PAAm SN hydrogels. (b) Force−extension curves of unfolding CPS nanospheres in deionized water. The blue line is the force−extension curve. The red curve is the WLC fitting to the elastic stretching part. The black line is the baseline. (c) AFM image shows the CPS nanosphere structure with a height of 2−8 nm. (d) SEM images of the PS/PAAm DN hydrogel at different magnifications. Optical images of the PS/PAAm DN hydrogel before (e) and after (f) the stretching.

was immersed in a 60 °C oil batch for 80 h to conduct polymerization with a moderate conversion rate. After cooling to room temperature, THF was added to the tube to dissolve the CPS. The diluted solution was dropwise added to a stirring cold MeOH solution to precipitate polystyrene three times. The precipitate was collected and dried before use.

2.3. Synthesis of PS/PAAm DN Hydrogel. The PS/PAAm DN hydrogel was fabricated with the classical chemical cross-linking method.[45] The first network of the PS/PAAm DN hydrogel was synthesized from a DMF solution of 25 mM CPS containing 50 mol % (with respect to CPS) cross-linking agent, 4-armed-PEG-NH_2, and 66 mol % (with respect to CPS) activator, HBTU, in the reaction cell consisting of a pair of glass plates with 1 mm spacing; 4 mol % (with respect to CPS) TEA was evenly added into it. After polymerization, the hydrogel was immersed in a large amount of DMSO for 1 week to equilibrate and to wash away the residual chemicals. This first network hydrogel was then immersed in a DMSO solution of 2 M AAm, containing 1 mol % (with respect to AAm) cross-linking agent, MBAA, and 0.1 mol % (with respect to AAm) photoinitiator, phenyl bis(2,4,6-trimethylbenzoyl)-phosphine oxide, in the reaction cell and was purged with argon gas for 30−45 min and irradiated with UV light (285 nm, 2000 mW cm^{-2}) for 5 h at 25 °C. After polymerization, the PS/PAAm DN hydrogel was immersed in a large amount of deionized water for 1 week to equilibrate. The cross-linking density is defined as the molar fraction ratio of the cross-linking agent to monomer concentration. We obtained the PS/PAAm DN hydrogel with the first and second networks; it had cross-linking densities of 50 and 1%, respectively.

2.4. Single-Molecule Force Spectroscopy. Silicon nitride (Si_3N_4) cantilevers (Type: MLCT-D, Bruker) with typical spring constants of ∼50 pN/nm were used for all SMFS experiments. The cantilevers and substrates were pretreated with amino-functionalized polyethylene glycol to minimize the possible nonspecific adsorption of CPS to the cantilever tip and to allow the formation of amide adducts with the carboxyl at the end of the surface-anchored CPS polymers. The cantilevers and substrates were first immersed in a chromic acid solution at 80 °C for 0.5 h. Next, the cantilevers and substrates were washed extensively with water and then ethanol and kept dry. Then, the cantilevers were functionalized with the amino group in 1% (v/v) APTES in toluene for 1 h, and the substrates were cross-linked with the carboxyl group in 8 mg/mL of CPS solution with 80% (v/v) TEA for 6 h. The amino-coated cantilevers and substrates were extensively washed with THF and then ethanol and kept dry before being used in the SMFS experiments. Note that because the cantilevers and substrates were functionalized with amino groups, the nonspecific interactions of the cantilever tip and the CPS molecules were markedly reduced.

2.5. ^{1}H Nuclear Magnetic Resonance and Fourier Transform Infrared Spectroscopy. The ^{1}H NMR spectrum of CPS was measured on a DRX (Germany, Bruker) 500 MHz spectrometer using DMSO-d_6 as the solvent. The FTIR spectrum of the PS/PAAm DN hydrogel, PS, and PAAm SN hydrogel were revealed by NEXUS870 (the United States of America, Nicolet). Measurements were recorded between 4000 and 400 cm^{-1}.

2.6. Scanning Electron Microscopy and Rheology Test. SEM images were obtained using a S-3400N scanning

https://doi.org/10.1021/acsomega.3c01813
ACS Omega 2023, 8, 35619−35627

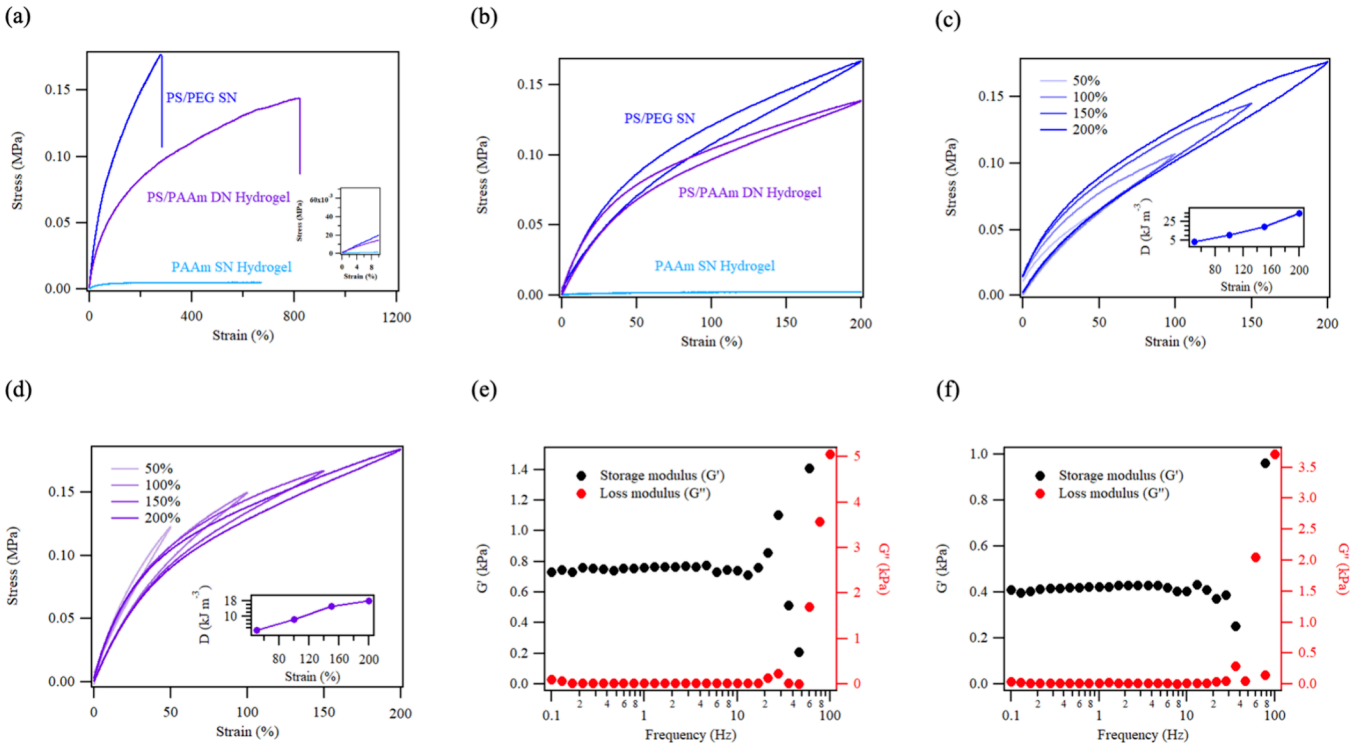

Figure 3. Mechanical properties of the PS/PAAm DN hydrogels. (a) Stress−strain curves of the three types of hydrogels, with each stretching to rupture. Illustration shows the strain at 10%. (b) Each hydrogel is loaded to a strain of 200%, just below the value that ruptures PS/PEG SN, and is then unloaded. Samples of the PS/PEG SN (c) and PS/PAAm DN hydrogels (d) are subjected to a cycle of loading and unloading of varying maximum strain (50, 100, 150, and 200%). Illustration shows the energy dissipation of the PS/PEG SN and PS/PAAm DN hydrogels under the corresponding strain, respectively. Frequency sweep of the storage modulus (G') and loss modulus (G'') of the PS/PEG SN (e) and PS/PAAm DN hydrogels (f), respectively.

electron microscope (Japan, Hitachi) at 20 kV. All of the hydrogels were lyophilized and Au-sputter-coated prior to the measurement. We used a rheometer (HAAKE RS600) equipped with a cycle plate geometry of 50 mm diameter. The truncation gap was set to 0.5 mm. Before the measurement, the instrument inertia was checked, and the system was calibrated, as is routine. 1 mL of sample was placed on the temperature-controlled plate at 30 °C. The cycle plate was set at the measuring position, and excess sample was trimmed. The following tests were performed in triplicate: strain sweeps were performed at an oscillatory frequency of 1 Hz and shear strain ranging from 0.1 to 1000%. One hundred data points were collected over the linear-scale range of shear strain values. Frequency sweeps were performed between 0.1 and 100 Hz at 1% shear strain. Twenty-eight data points were collected for each measurement.

2.7. Mechanical Test. The tensile test was carried out using a commercial test machine (Instron-5944 with a 10 N sensor) in air at room temperature. The rate of tension was kept as 20% min^{-1} (~1 mm min^{-1}) with respect to the original height of the hydrogel. Young's modulus corresponded to the approximate linear fitting value in a strain of 0−10%. The toughness was calculated from the area below the stress−strain curve until fracture. The fracture energy was calculated with $G = \frac{F_{ave}}{W}$, where F_{ave} is the tearing resistance force and W is the width of the hydrogel.[46] The recovery percentage was defined as the normalized maximum stress, with the initial maximum stress as 100% after the continuous stretching−relaxation cycles for hydrogels. All of the results are the average of three tests.

2.8. Measurement of Water Content. The surface water of a swollen equilibrium hydrogel was carefully wiped using a filter paper, and W_0 was measured. The temperature of the drying oven was set as 80 °C for 2 days, and the final weight W_d was obtained.

$$\text{Water Content} = \frac{(W_0 - W_d)}{W_0} \times 100\%$$

2.9. Statistical Analysis. All data were presented as mean ± standard deviation (SD) and evaluated using an unpaired Student's t test. Statistical analysis was performed using IGOR Pro 6.37 software (WaveMetrics Inc., OR, USA).

3. RESULTS AND DISCUSSION

3.1. Characterization of the PS/PAAm DN Hydrogels. We first employ the FTIR spectra to analyze the chemical structure of the PS/PAAm DN hydrogel, PAAm SN hydrogel, and PS (Figure 2a). As we can see from Figure 2a, the bands around the PS/PAAm DN hydrogel and PAAm SN hydrogel appear at 1655 cm^{-1}, corresponding to −C═O− on the peptide bond, and the bands around PS/PAAm DN hydrogel and PS appear at 696 cm^{-1}, corresponding to −C−H− on the benzene ring. We consider that the carboxyl group on CPS and the amino group on 4-armed-PEG-NH_2 can covalently cross-link to form a rigid network for the PS/PAAm DN hydrogel. In addition, the ^1H NMR spectrum could also confirm our results (Figure S2, Supporting Information). All the peaks can be assigned as follows: δ: 0.9 (m, 3H, $-CH_3$), 1.3 (m, 2H, $-CH_2-$), 1.5 (m, 1H, $-CH\equiv$), 2.7 (m, 2H, $-CH_2-$ COOH), 3.4 (m, 2H, $-S-CH_2-$), 5.2 (m, 1H, − $S-C_6H_5-$

https://doi.org/10.1021/acsomega.3c01813
ACS Omega 2023, 8, 35619−35627

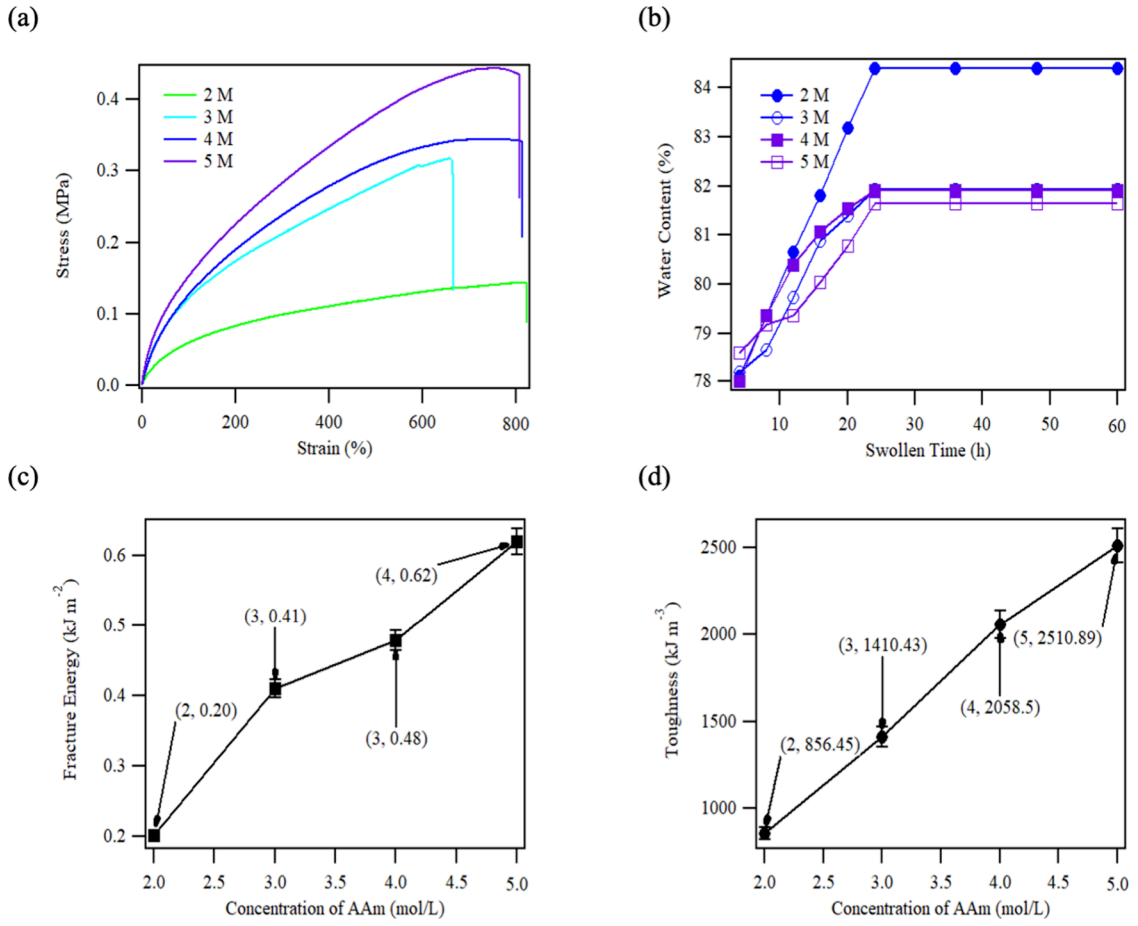

Figure 4. Stress−strain curves (a), water content (b), fracture energy (c), and toughness (d) of the PS/PAAm DN hydrogels with different concentrations of AAm. The cross-linking density remains the same.

CH−), and 6.6−7.2 (m, 5H, $-C_6H_5-$). Based on the above data, we demonstrate that we have successfully added the carboxyl groups to PS. To characterize how the stretching process of CPS affects the property of the PS/PAAm DN hydrogels, second, we measure the force−extension curve of the CPS using atomic force spectroscopy (AFM)-based SMFS in air at room temperature. AFM-based SMFS technology is helpful to establish the relationship between the chain structure, chain composition, and single-chain elasticity of synthetic polymers and the interaction between chains and their macromechanical properties and to understand the relationship between the structure and interaction of biological macromolecules and their biological functions.[47−50] Figure 2b shows the typical force−extension curve of the unfolding CPS nanosphere in water (blue line). Driven by hydrophobic interactions, the CPS collapses into a compact nanospherical structure at the beginning of the force−extension curves.[51] The long force plateau indicates that the unfolding nanosphere is under constant force before the collapsed nanosphere transforms into a fully extended chain. The rupture peak shows that the extended chain is further stretched until a certain chemical bond breaks. This stretching process can be well fitted by the worm-like chain (WLC) model (red line).[52,53] The CPS attaches to the monocrystalline silicon wafer in water, showing a nanosphere structure with a height of 2−8 nm by AFM imaging (Figure 2c). In order to clarify the microstructure, we next employ the SEM observation of a PS/PAAm DN hydrogel after freeze-drying. The high glass-transition temperature (T_g) of CPS and PAAm (80, 188 °C) can maintain the structure after the dehydration of the DN hydrogel, which makes it suitable for structure observation. The SEM images reveal that some porous 3D networks exist in the PS/PAAm DN hydrogel (Figure 2d). The PS/PAAm DN hydrogel can be stretched to 8 times its original length without rupture (Figure 2e,f); mechanical tests are performed in air at room temperature using a tensile machine with a 10 N load cell. In both loading and unloading, the rate of stretching is kept constant at 1 mm min^{-1}.

3.2. Mechanical Properties of the PS/PAAm DN Hydrogels. We chose 25 mM CPS to construct the PS/PAAm DN hydrogels because it has superior mechanical properties than that of 10 and 30 mM CPS (Figure S3, Supporting Information). The PS/PAAm DN hydrogels are even more remarkable when compared with their parents, the PS/PEG SN and PAAm SN hydrogels (Figure 3a). The molar concentrations of CPS and AAm in the PS/PAAm DN hydrogels are kept the same as those in the PS/PEG SN and PAAm SN hydrogels, respectively. When the elongation is small (3.9% strain), the Young's modulus of the PS/PAAm DN hydrogel is 222.05 kPa, which is close to the Young's modulus of PS/PEG SN (219.27 kPa). The maximum strength and fracture strain are, respectively, 143 and 820% for the PS/PAAm DN hydrogel, 177 and 280% for the PS/PEG SN hydrogel, and 5 and 670% for the PAAm SN hydrogel. Thus, the fracture strain of the PS/PAAm DN hydrogels exceeds

https://doi.org/10.1021/acsomega.3c01813
ACS Omega 2023, 8, 35619−35627

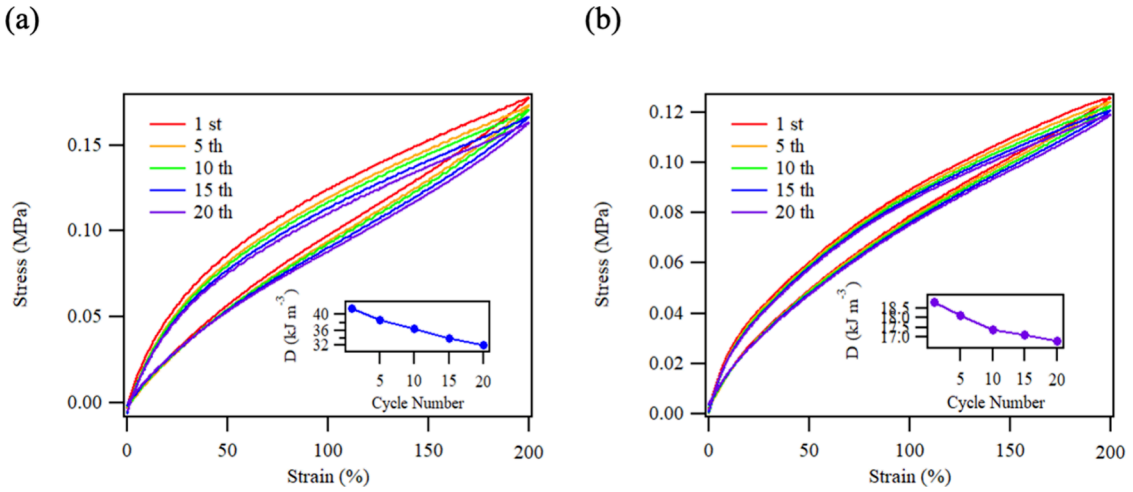

Figure 5. Recoverability of the PS/PAAm DN hydrogels. After the first cycle of loading and unloading of the PS/PEG SN (a) and PS/PAAm DN hydrogels (b), one sample is immediately reloaded 20 times. Illustration shows the energy dissipation of the PS/PEG SN and PS/PAAm DN hydrogels under the corresponding number of cycles, respectively.

those of either of its parents, and the fracture stress far surpasses the PAAm SN hydrogels.

The PS/PEG SN hydrogel effectively dissipates more energy than does the PS/PAAm DN hydrogel. The area between the loading and unloading curves of a hydrogel gives the energy dissipated per unit volume. Figure 3b shows that the PS/PEG SN and PS/PAAm DN hydrogels have different energy dissipation at 200% strain, that is, 33.89 and 17.81 kJ m^{-3}, respectively. Next, we study the energy dissipation of PS/PEG SN and PS/PAAm DN hydrogels at different strains (50, 100, 150, and 200%). Figure 3c shows the stress−strain curves of PS/PEG SN at different strain rates. It is clear that the energy dissipation of PS/PEG SN increases with the increase of strain (from 3.21 to 33.89 kJ m^{-3} in the illustration). PS/PEG SN exhibits pronounced hysteresis and retains significant permanent deformation after unloading. In contrast, the PAAm SN hydrogel fully recovers its original length after unloading due to the low energy dissipation (Figure 3b). The PS/PAAm DN hydrogel also shows hysteresis, but the permanent deformation after unloading is significantly smaller than that of the PS/PEG SN hydrogel. Figure 3d shows the stress−strain curves of the PS/PAAm DN hydrogel at different strain rates. It is clear that the energy dissipation of PS/PAAm DN hydrogels also increases with the increase of strain (from 2.82 to 17.81 kJ m^{-3} in the illustration) but is smaller than that of the PS/PEG SN hydrogel. We suppose that PAAm SN makes the PS/PAAm DN hydrogel tougher and closer to the elastomer than PS/PEG SN, and the energy dissipation gradually increases with the strain, suggesting that more cross-linkers would rupture at a large strain. Rheological studies (Figure 3e,f) show that both PS/PEG SN and PS/PAAm DN hydrogels have the storage modulus (G') and loss modulus (G'') in which $G' > G''$, and G' of PS/PEG SN is twice as that of the PS/PAAm DN hydrogel. We consider that the PS/PAAm DN hydrogel is a softer hydrogel.

Furthermore, the cross-linking density of the second network, that is, the concentration of MBAA (Figure S4, Supporting Information), and the stretch rate (Figure S5, Supporting Information) also strongly affect the mechanical behavior of the PS/PAAm DN hydrogels. We consider that the mechanical properties of PS/PAAm DN hydrogels are weakened due to the low density when the concentration of CPS is 10 mM because the first network provides rigidity to the PS/PAAm DN hydrogels;[2] on the contrary, when the concentration of CPS is 30 mM, the mechanical properties of PS/PAAm DN hydrogels are also weakened due to the "wind" or "knot" of the redundant polymer molecular chains. Meanwhile, the strength of PS/PAAm DN hydrogels is enhanced with the increased cross-linking density of the second network, which provides ductility to the PS/PAAm DN hydrogels.[2] The higher the cross-linking density of the second network of PS/PAAm DN hydrogels, the greater is its strength and the smaller its elongation. If the cross-linking density of the second network is higher than 1 mol %, the strength of PS/PAAm DN hydrogels increases while the elongation decreases. Till now, we can make a conclusion that the PS/PAAm DN hydrogels have the best mechanical properties when the concentration of CPS is 25 mM and the cross-linking density of the second network is 1 mol %.

Besides, we prepare the PS/PAAm DN hydrogels containing various concentrations of AAm (2, 3, 4, and 5 M) to study why the DN hydrogels are much more stretchable than either of their parents. When the concentration of AAm is increased from 2 to 5 M, the strength of PS/PAAm DN hydrogels increases from 0.14 to 0.43 MPa, respectively (Figure 4a). We consider that the mechanical properties of PS/PAAm DN hydrogels are enhanced owing to the raised concentration of AAm.[2] However, the water content of PS/PAAm DN hydrogels decreases with the increase in AAm (Figure 4b). The PS/PAAm DN hydrogel is soaked in water for 24 h to reach the swelling equilibrium, and the water content decreases from 84.39% at 2 M to 81.64% at 5 M. We suppose that the three-dimensional structure of PS/PAAm DN hydrogels is too small with the increased cross-linking density to contain water. The fracture energy reaches a maximum value of 0.62 kJ m^{-2} at 5 M acrylamide (Figure 4c), and the toughness reaches 2510.89 kJ m^{-3} (Figure 4d). When the concentration of CPS increases from 10 to 30 mM, the fracture energy of the PS/PAAm DN hydrogels increases from 0.079 to 0.151 kJ m^{-2} (Table 1, Supporting Information). At the same time, when the covalent cross-linking density of the second network changes from 0.5 to 2 mol %, the fracture energy of the PS/PAAm DN hydrogels changes from 0.127 to 0.190 kJ m^{-2} (Table 2, Supporting Information).

https://doi.org/10.1021/acsomega.3c01813
ACS Omega 2023, 8, 35619−35627

3.3. Mechanical Recoverability of the PS/PAAm DN Hydrogels. Next, we studied the recoverability of the PS/PAAm DN hydrogels. The PS/PEG SN (Figure 5a) and PS/PAAm DN hydrogels (Figure 5b) are subjected to 20 stretching−relaxation cycles without interval. The results show that the conformation of PS/PEG SN becomes 92.7% of its initial state after 20 consecutive stretching−relaxation cycles (Figure S6, Supporting Information), its energy dissipation is reduced by 21.8% (from 41.5 to 32.45 kJ m^{-3}), and the maximum strength is reduced by 7.3% (from 0.178 to 0.165 MPa), which is caused by the covalently cross-linked network structure, while for the PS/PAAm DN hydrogel, the conformation becomes 94.5% of its initial state (Figure S7, Supporting Information), its energy dissipation is reduced by 10.5% (from 18.79 to 16.82 kJ m^{-3}), and the maximum strength is reduced by 5.5% (from 0.144 to 0.136 MPa).

4. CONCLUSIONS

Our experimental findings provide insights into the mechanisms of deformation and energy dissipation in these hydrogels. When the PS/PAAm DN hydrogel is subjected to a small stretch, the Young's modulus of the PS/PAAm DN hydrogel is nearly close to that of PS/PEG SN. Thus, the polystyrene chains bear loads at the beginning of stretching in the PS/PAAm DN hydrogel. The load sharing of the two networks may be achieved by entanglements of the polymers and by the covalent cross-links formed between the amino groups on PEG chains and the carboxyl groups on PS chains (Figure 1). Our data demonstrate that the PS/PAAm DN hydrogels consisting of polystyrene nanospheres have the ability to be elongated under an external force. When the external force is removed, it can be restored to approximately its original state (94.5%). The chemically cross-linked network structures make the DN hydrogels have high mechanical properties. Our experiment provides a new idea for the design of a fully chemically cross-linked DN hydrogel with recoverability and also provides a wider platform for the application of hydrophobic polymers.

■ ASSOCIATED CONTENT

Supporting Information

The Supporting Information is available free of charge at https://pubs.acs.org/doi/10.1021/acsomega.3c01813.

Weight-average molecular weight (Mw), number-average molecular weight (Mn), and polydispersity quantified by gel permeation chromatography; 1H NMR spectrum of CPS; strain-stress curves of the PS/PAAm DN hydrogels at different concentrations of CPS and MBAA and at different stretch rates; energy dissipation and recovery percentage curves of the PS/PEG SN and PS/PAAm DN hydrogels; and different mechanical properties of the PS/PAAm DN hydrogels with various concentrations of CP (PDF)

■ AUTHOR INFORMATION

Corresponding Authors

Zhongying Jiang − *Key Laboratory of Micro-nano Electric Sensing Technology and Bionic Devices, Department of Network Security and Information Technology, Yili Normal University, Yining 835000, P. R. China*; orcid.org/0009-0003-1615-8478; Email: jiangzhying@163.com

Jie Sheng − *Department of Electronics and Engineering, Yili Normal University, Yining 835000, P. R. China*; Email: shj1595@163.com

Authors

Runda Wang − *Key Laboratory of Micro-nano Electric Sensing Technology and Bionic Devices, Department of Network Security and Information Technology and Department of Electronics and Engineering, Yili Normal University, Yining 835000, P. R. China*

Yiteng Lei − *Department of Electronics and Engineering, Yili Normal University, Yining 835000, P. R. China*

Tao Zhu − *National Key Laboratory of Solid State Microstructures, Department of Physics, Nanjing University, Nanjing 210093, P. R. China*

Rong Fan − *Department of Electronics and Engineering, Yili Normal University, Yining 835000, P. R. China*

Complete contact information is available at: https://pubs.acs.org/10.1021/acsomega.3c01813

Author Contributions

The manuscript was written through contributions of all authors. All authors have given approval to the final version of the manuscript.

Funding

This research was funded by Nature Science Foundation of Xinjiang Uygur Autonomous Region (2022D01C336), YiLi Normal University's Special Self Research Key Project to Enhance the Comprehensive Strength of Disciplines (22XKZZ07), the National Natural Science Foundation of China (22163011 and 12227808), YiLi Normal University's "High-level Talents" Program of Academic Integrity (YSXSDTR22002), and YiLi Normal University's "Scientific Research" Program (YS2022G002).

Notes

The authors declare no competing financial interest.

■ ACKNOWLEDGMENTS

All authors thank Ph. D. Yi Cao for experimental instructions and data analysis.

■ REFERENCES

(1) Ullah, F.; Othman, M. B. H.; Javed, F.; Ahmad, Z.; Md Akil, H. Classification, Processing and Application of Hydrogels: A Review. *Mater. Sci. Eng., C* **2015**, *57*, 414−433.

(2) Gong, J. P.; Katsuyama, Y.; Kurokawa, T.; Osada, Y. Double-Network Hydrogels with Extremely High Mechanical Strength. *Adv. Mater.* **2003**, *15*, 1155−1158.

(3) Lam, J.; Clark, E. C.; Fong, E. L. S.; Lee, E. J.; Lu, S.; Tabata, Y.; Mikos, A. G. Evaluation of Cell-Laden Polyelectrolyte Hydrogels Incor-porating Poly(L-Lysine) for Applications in Cartilage Tissue Engineering. *Biomaterials* **2016**, *83*, 332−346.

(4) Lee, K. Y.; Mooney, D. J. Hydrogels for Tissue Engineering. *Chem. Rev.* **2001**, *101*, 1869−1879.

(5) Yang, F.; Guo, G.; Wang, Y. Inflammation-Triggered Dual Release of Nitroxide Radical and Growth Factor from Heparin Mimick-ing Hydrogel-Tissue Composite as Cardiovascular Implants for Anti-Coagulation, Endothelialization, Anti-Inflammation, and Anti-Calcification. *Biomaterials* **2022**, *289*, 121761.

(6) Qiu, Y.; Park, K. Environment-Sensitive Hydrogels for Drug Delivery. *Adv. Drug Delivery Rev.* **2001**, *53*, 321−339.

(7) Hu, X.; Gong, X. A New Route to Fabricate Biocompatible Hydrogels with Controlled Drug Delivery Behavior. *J. Colloid Interface Sci.* **2016**, *470*, 62−70.

(8) Huebsch, N.; Kearney, C. J.; Zhao, X.; Kim, J.; Cezar, C. A.; Suo, Z.; Mooney, D. J. Ultrasound-Triggered Disruption and Self-Healing of Reversibly Cross-Linked Hydrogels for Drug Delivery and Enhanced Chemotherapy. *Proc. Natl. Acad. Sci. U. S. A.* **2014**, *111*, 9762−9767.
(9) Discher, D. E.; Mooney, D. J.; Zandstra, P. W. Growth Factors, Matrices, and Forces Combine and Control Stem Cells. *Science* **2009**, *324*, 1673−1677.
(10) Ma, M.; Guo, L.; Anderson, D. G.; Langer, R. Bio-Inspired Polymer Composite Actuator and Generator Driven by Water Gradients. *Science* **2013**, *339*, 186−189.
(11) Tokarev, I.; Minko, S. Stimuli-Responsive Porous Hydrogels at Interfaces for Molecular Filtration, Separation, Controlled Release, and Gating in Capsules and Membranes. *Adv. Mater.* **2010**, *22*, 3446−3462.
(12) Jiang, H.; Duan, L.; Ren, X.; Gao, G. Hydrophobic Association Hydrogels with Excellent Mechanical and Self-healing Properties. *Eur. Polym. J.* **2019**, *112*, 660−669.
(13) Metters, A. T.; Anseth, K. S.; Bowman, C. N. Fundamental Studies of A Novel, Biodegradable PEG-b-PLA Hydrogel. *Polymer* **2000**, *41*, 3993−4004.
(14) Gu, J.; Guo, Y.; Li, Y.; Wang, J.; Wang, W.; Cao, Y.; Xue, B. Tuning Strain Stiffening of Protein Hydrogels by Charge Modification. *Int. J. Mol. Sci.* **2022**, *23*, 3032.
(15) Yu, W.; Sun, W.; Chen, H.; Wang, J.; Xue, B.; Cao, Y. Gradual Stress-Relaxation of Hydrogel Regulates Cell Spreading. *Int. J. Mol. Sci.* **2022**, *23*, 5170.
(16) Han, Y.; Liu, C.; Xu, H.; Cao, Y. Engineering Reversible Hydrogels for 3D Cell Culture and Release Using Diselenide Catalyzed Fast Disulfide Formation. *Chin. J. Chem.* **2022**, *40*, 1578−1584.
(17) Ito, K. Novel Cross-Linking Concept of Polymer Network: Synthesis, Structure, and Properties of Slide-Ring Gels with Freely Movable Junctions. *Polym. J.* **2007**, *39*, 489−499.
(18) Haraguchi, K.; Takehisa, T. Nanocomposite Hydrogels: A Unique Organic−inorganic Network Structure with Extraordinary Mechanical, Optical, and Swelling/de-swelling Properties. *Adv. Mater.* **2002**, *14*, 1120−1124.
(19) Jiang, G.; Liu, C.; Liu, X.; Zhang, G.; Yang, M.; Liu, F. Construction and Properties of Hydrophobic Association Hydrogels with High Mechanical Strength and Reforming Capability. *Macromol. Mater. Eng.* **2009**, *294*, 815−820.
(20) Huang, T.; Xu, H. G.; Jiao, K. X.; Zhu, L. P.; Brown, H. R.; Wang, H. L. A Novel Hydrogel with High Mechanical Strength: A Macromolecular Microsphere Composite Hydrogel. *Adv. Mater.* **2007**, *19*, 1622−1626.
(21) Li, C.; Rowland, M. J.; Shao, Y.; Cao, T.; Chen, C.; Jia, H.; Zhou, X.; Yang, Z.; Scherman, O. A.; Liu, D. Responsive Double Network Hydrogels of Interpenetrating DNA and CB[8] Host−Guest Supramolecular Systems. *Adv. Mater.* **2015**, *27*, 3298−3304.
(22) Li, X.; Wu, C.; Yang, Q.; Long, S.; Wu, C. Low-Velocity Super-Lubrication of Sodium-Alginate/Polyacrylamide Ionic-Covalent Hybrid Double-Network Hydrogels. *Soft Matter* **2015**, *11*, 3022−3033.
(23) Wang, T.; Zhang, Y.; Gu, Z.; Cheng, W.; Lei, H.; Qin, M.; Xue, B.; Wang, W.; Cao, Y. Regulating Mechanical Properties of Poly-mer-Supramolecular Double-Network Hydrogel by Supramolecular Self-Assembling Structures. *Chin. J. Chem.* **2021**, *39*, 2711−2717.
(24) Li, L.; Zhang, K.; Wang, T.; Wang, P.; Xue, B.; Cao, Y.; Zhu, L.; Jiang, Q. Biofabrication of a Biomimetic Supramolecular-Polymer Double Network Hydrogel for Cartilage Regeneration. *Mater. Des.* **2020**, *189*, 108492.
(25) Nasim, G.; Hamidreza, G.; Mahshid, K.; Monhammadhossein, F. A Facile One-Step Strategy for Development of a Double Network Fibrous Scaffold for Nerve Tissue Engineering. *Biofabrication* **2017**, *9*, No. 025008.
(26) Gong, J. P. Materials Both Tough and Soft. *Science* **2014**, *344*, 161−162.
(27) Sun, J.-Y.; Zhao, X.; Illeperuma, W. R. K.; Chaudhuri, O.; Oh, K. H.; Mooney, D. J.; Vlassak, J. J.; Suo, Z. Highly Stretchable and Tough Hydrogels. *Nature* **2012**, *489*, 133−136.
(28) Hu, J.; Hiwatashi, K.; Kurokawa, T.; Liang, S. M.; Wu, Z. L.; Gong, J. P. Microgel-Reinforced Hydrogel Films with High Mechanical Strength and Their Visible Mesoscale Fracture Structure. *Macromolecules* **2011**, *44*, 7775−7781.
(29) Nakajima, T.; Furukawa, H.; Tanaka, Y.; Kurokawa, T.; Gong, J. P. Effect of Void Structure on the Toughness of Double Network Hy-drogels. *J. Polym. Sci., Part B: Polym. Phys.* **2011**, *49*, 1246−1254.
(30) Suekama, T.; Hu, J.; Kurokawa, T.; Gong, J.; Gehrke, S. Double-Network Strategy Improves Fracture Properties of Chon-droitin Sul-fate Networks. *ACS Macro Lett.* **2013**, *2*, 137−140.
(31) Gong, J. P. Why Are Double Network Hydrogels so Tough? *Soft Matter* **2010**, *6*, 2583−2590.
(32) Yao, C.; Liu, Z.; Yang, C.; Wang, W.; Ju, X.-J.; Xie, R.; Chu, L.-Y. Smart Hydrogels: Poly(N-Isopropylacrylamide)-Clay Nanocomposite Hydrogels with Responsive Bending Property as Temperature-Controlled Manipulators (Adv. Funct. Mater. 20/2015). *Adv. Funct. Mater.* **2015**, *25*, 3104−3104.
(33) Zakharchenko, S.; Ionov, L. Anisotropic Liquid Microcapsules from Biomimetic Self-Folding Polymer Films. *ACS Appl. Mater. Interfaces* **2015**, *7*, 12367−12372.
(34) Chen, P.; Wu, R.; Wang, J.; Liu, Y.; Ding, C.; Xu, S. One-Pot Preparation of Ultrastrong Double Network Hydrogels. *J. Polym. Res.* **2012**, *19*, 1−4.
(35) Li, J.; Suo, Z.; Vlassak, J. J. Stiff,Strong, and Tough Hydrogels with Good Chemical Stability. *J. Mater. Chem. B* **2014**, *2*, 6708−6713.
(36) Jiang, G.; Liu, C.; Liu, X.; Zhang, G.; Yang, M.; Liu, F. Construction and Properties of Hydrophobic Association Hydrogels with High Mechanical Strength and Reforming Capability. *Macromol. Mater. Eng.* **2009**, *294*, 815−820.
(37) Cui, J.; Lackey, M. A.; Madkour, A. E.; Saffer, E. M.; Griffin, D. M.; Bhatia, S. R.; Crosby, A. J.; Tew, G. N. Synthetically Simple, Highly Resilient Hydrogels. *Biomacromolecules* **2012**, *13*, 584−588.
(38) Cui, J. L.; Lackey, M. A.; Tew, G. N.; Crosby, A. Mechanical Properties of End-Linked PEG/PDMS Hydrogels. *Macromolecules* **2012**, *45*, 6104−6110.
(39) Yoon, J. W.; Park, Y.; Kim, J.; Park, C. H. Multi-Jet Electrospinning of Polystyrene/Polyamide 6 Blend: Thermal and Mechanical Properties. *Fash. Text.* **2017**, *4*, 9.
(40) Uyar, T.; Besenbacher, F. Electrospinning of Uniform Polystyrene Fibers: The Effect of Solvent Conductivity. *Polymer* **2008**, *49*, 5336−5343.
(41) Kobayashi, M.; Agari, R.; Kigo, Y.; Terada, A. Efficient Oxygen Supply and Rapid Biofilm Formation by a New Composite Polystyrene Elastomer Membrane for Use in a Membrane-Aerated Biofilm Reactor. *Biochem. Eng. J.* **2022**, *183*, 108442.
(42) Li, L.; Jiang, R.; Chen, J.; Wang, M.; Ge, X. In situ synthesis and self-reinforcement of polymeric composite hydrogel based on particulate macro-RAFT agents. *RSC Adv.* **2017**, *7*, 1513−1519.
(43) Lansalot, M.; Davis, T. P.; Heuts, J. P. A. RAFT Miniemulsion Polymerization: Influence of the Structure of the RAFT Agent. *Macromolecules* **2002**, *35*, 7582−7591.
(44) Puts, G.; Venner, V.; Améduri, B.; Crouse, P. Conventional and RAFT Copolymerization of Tetrafluoroethylene with Isobutyl Vinyl Ether. *Macromolecules* **2018**, *51*, 6724−6739.
(45) Chen, Q.; Chen, H.; Zhu, L.; Zheng, J. Fundamentals of Double Network Hydrogels. *J. Mater. Chem. B* **2015**, *3*, 3654−3676.
(46) Nakajima, T.; Hidemitsu, F.; Yoshimi, T.; Takayuki, K.; Yoshihito, O.; Gong, J. True Chemical Structure of Double Network Hydrogels. *Macromolecules* **2009**, *42*, 2184−2189.
(47) Zhang, J.; Lei, H.; Qin, M.; Wang, W.; Cao, Y. Quantifying cation-π interactions in marine adhesive proteins using single-molecule force spectroscopy. *Superamol. Mater.* **2022**, *1*, 100005.
(48) Lei, H.; Zhang, J.; Li, Y.; Wang, X.; Qin, M.; Wang, W.; Cao, Y. Histidine-Specific Bioconjugation for Single-Molecule Force Spectroscopy. *ACS Nano* **2022**, *16*, 15440−15449.

https://doi.org/10.1021/acsomega.3c01813
ACS Omega 2023, 8, 35619−35627

(49) Shi, S.; Wang, Z.; Deng, Y.; Tian, F.; Wu, Q.; Zheng, P. Combination of Click Chemistry and Enzymatic Ligation for Stable and Efficient Protein Immobilization for Single-Molecule Force Spectroscopy. *CCS Chem.* **2022**, *4*, 598−604.
(50) Yin, Z.; Song, G.; Jiao, Y.; Zheng, P.; Xu, J. F.; Zhang, X. Dissipative Supramolecular Polymerization Powered by Light. *CCS Chem.* **2019**, *1*, 335−342.
(51) Di, W.; Wang, X.; Zhou, Y.; Mei, Y.; Wang, W.; Cao, Y. Fluorination Increases Hydrophobicity at the Macroscopic Level but Not at the Microscopic Level. *Chin. Phys. Lett.* **2022**, *39*, No. 038701.
(52) Marko, J. F.; Siggia, E. D. Stretching DNA. *Macromolecules* **1995**, *28*, 8759−8770.
(53) Bao, Y.; Luo, Z.; Cui, S. Environment-Dependent Single-Chain Mechanics of Synthetic Polymers and Biomacromolecules by Atomic Force Microscopy-Based Single-Molecule Force Spectroscopy and the Implications for Advanced Polymer Materials. *Chem. Soc. Rev.* **2020**, *49*, 2799−2827.

https://doi.org/10.1021/acsomega.3c01813
ACS Omega 2023, 8, 35619−35627